Introduction to Medical Image Analysis
2019-2020

Population Shape Regression from Random Design Data

Ariane Alix
Antoine de Reviers
Raphaël Ginoulhac

Elèves ingénieurs, Master MVA

---

1 Abstract (Ariane)

This report will analyze the paper named "Population Shape Regression from Random Design Data" and the method presented in it, authored by B. Davis, P. Thomas Fletcher, E. Bullitt, and S. Joshi. This paper aims to study anatomical shape changes, in particular of the human brain, as a function of age. Since classical regression technics use flat Euclidean spaces, they are not able to represent the natural variability of the human anatomy. Therefore, the method developed in this paper applies regression methods to manifold-valued data (the infinite dimensional manifold of diffeomorphic transformations) that will better represent the reality.

We will try to analyze the article from a critical point of view, and assess the improvement it brought from the state of the art at the time of its publication (2010). We will also describe potential applications and introduce some examples of more recent related methods.

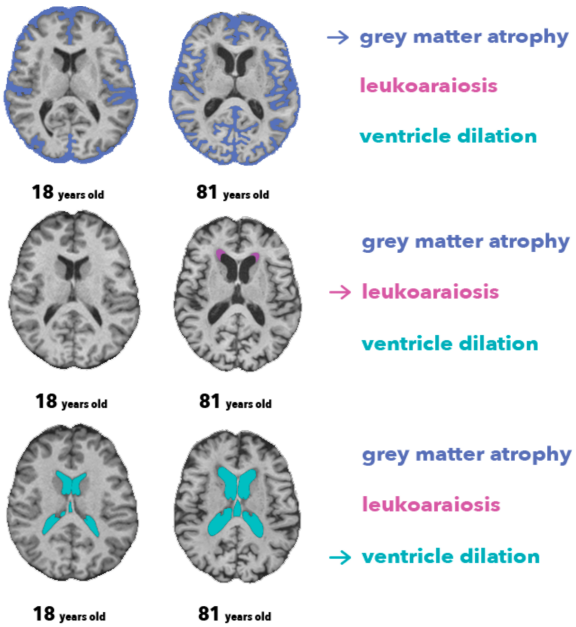

Figure 1: Evolution of the brain with aging– Source: [17]

2 Introduction (Antoine)

This article aims to build a growth model in order to quantify the evolution of the shape of the brain as a function of the age.

2.1 Growth models before publication of the article

Growth models had already been applied to medical imaging for various topics. For instance, Clatz et al. 2005 [1] provide a model to study the 3-dimensional growth of a glial tumor, the glioblastomas multiforma, as well as Swanson et al. 2000 [2] for gliomas in grey and white matter. Many studies have been made with a similar model but theses approaches study the density of the tumor mainly, so it can not be directly applied in our case where we need to follow the geometric shape deformation.

Thompson et al. 2000 [3] also studies the brain development but for younger subjects (3 to 15 years old) using continuum mechanical tensor maps. Good results have been found with this method, but in a sense this case is easier because it focuses on subjects at an age where brain is developing a lot, so shape transformation is much more significant. In our case we want to study adults brains, so we need a more sensible analysis tool.

However, Miller 2004 [4] applies theory on groups of diffeomorphisms to study shape, growth, and atrophy of multiple types of medical images. The idea is to study the diffeomorphic flow g_t transforming an inital image I_0 into its shape I_t at time t by minimizing a particular distance between I_t and $I_0 \circ g_t^{-1}$. This kind of approach is much more relevant for our problem because we have seen that Riemmanian geometry allows a better analysis on shape transformation. This method constitutes the starting point for our model.

2.2 Extension provided by the article

The main issue with the above mentioned methods, and in particular the last one that appeared as the most relevant in our case, is that they use longitudinal models. This raises two issues :

- We need to collect instances at various times for every subject, which is very tough if we want to study a large range of age. In our case we study subjects from 20 to 79 years old, so it is almost impossible.
- Rather than creating a follow up for each subject, the article aims to build a global estimation of the shape of the brain as a function of time.

The last point leads us to search for a way to average deformation measures, or in other words to estimate an image I_t, at any time t, relevant to describe the shape of the brain at age t at the population scale. To that extent, the model of the article uses Kernel regression theory from Nadaraya 1964 [5] and Watson 1964 [6] and derives the Nadaraya-Watson estimator to Riemmanian manifold values instead of Euclidian space values. For that purpose, we need to have a distance defined on this manifold: we use again the distance introduced in Miller 2004 [4].

To sum up, we have a dataset $\mathcal{D} = \{t_i, I_i\}$, the distance $d_{\mathcal{I}}(I, J)$ and the Nadaraya-Watson estimator $\hat{I}_{NW}(t; \mathcal{D}, d_{\mathcal{I}})$ and we look for the flow g_t:

$$\underset{g}{\text{argmin}} \int_{t=0}^{T} d_{\mathcal{I}} \left(\hat{I}_{NW}(0) \circ g_t^{-1}, \hat{I}_{NW}(t) \right) dt$$

3 Analysis of the article

3.1 Algorithm

There are two main steps to the computation of the final model. The input data is a dataset of pairs of images (brain for example) and the associated age of the patient. Due to the huge variability of brain shape among a population, even of same age, we first need to harmonize the data by computing an "average" brain shape per age range before analyzing the correlation of deformation with aging.

3.1.1 Step 1 : Kernel Regression

This step is the one responsible for the computation of an average representative brain per age, and uses a method inspired from the averaging in metric spaces proposed by Fréchet.

3.1.1.1 Brief introduction to Kernel Regression methods (Ariane)

Kernel methods aim to find a relation (that may be non-linear), between pairs of random variables X and Y. They are non-parametric statistical methods, and are generally used for regressions. A bandwith coefficient h is associated, and regulates the smoothing of the approximation by determining the influence of distant Xs : the higher the h, the higher the influence of faraway points.
Example of application in 1D :

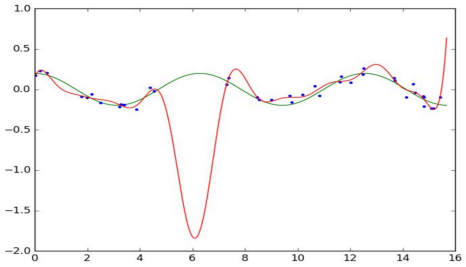

Figure 2: Kernel regression in 1 dimension

In red, h is small and the curve is closer to the points, but it is overfitting and therefore not representative of the trend we would like to analyze. In green, h is big and the result is smooth but with a higher accuracy error.

3.1.1.2 Nadaraya-Watson (Antoine)

The Nadaraya-Watson kernel regression – on which the method of the article is based – is a locally weighted average, using a kernel as the weighting function. Given a dataset $(t_i, y_i)_{i=1}^N$, we want to predict at any time t a dependant variable Y by $\mathbb{E}(Y|t) = m(t)$. In the univariate case, we consider Y as a vector of an euclidian space and the estimators $\widehat{m}_h$ can be written as :

$$\widehat{m}_h(t) = \frac{\sum_{i=1}^n K_h(t-t_i)y_i}{\sum_{j=1}^n K_h(t-t_j)}$$

where K_h is a kernel with a bandwidth h.

In our case, euclidian spaces are not relevant to describe anatomical shape transformations and we should rather search Y as a point on a Riemannian manifold $\mathcal{M}$. Therefore we use manifold-values $y_i = p_i \in \mathcal{M}$ and Fréchet expectation estimator:

$$\mu = \underset{q\in\mathcal{M}}{\operatorname{argmin}} \frac{1}{N}\sum_{i=1}^N d(q,p_i)^2$$

where $d(q,m)$ is the metric on $\mathcal{M}$. The estimators become :

$$\widehat{m}_h(t) = \underset{q\in\mathcal{M}}{\operatorname{argmin}} \left(\frac{\sum_{i=1}^n K_h(t-t_i)d(q,p_i)^2}{\sum_{j=1}^n K_h(t-t_j)} \right)$$

As we have seen previously, the choice of the kernel bandwidth h is critical : we need to regress from values close enough in time to get significant changes along the timeline and we also need to pick them far enough to have enough values and avoid being biased by eventual outliers. For that purpose, we use an estimator based on least squares cross-validation :

$$\hat{h} = \underset{h\in\mathbb{R}_+}{\operatorname{argmin}} \frac{1}{N}\sum_{i=1}^N d(\hat{m}_h^{i-}(t_i), p_i)^2$$

with

$$\hat{m}_h^{i-}(t) = \underset{q\in\mathcal{M}}{\operatorname{argmin}} \left(\frac{\sum_{j=1,j\neq i}^n K_h(t-t_j)d(q,p_j)^2}{\sum_{j=1,j\neq i}^n K_h(t-t_j)} \right)$$

3.1.2 Regression of Rotational Pose : SO(3) (Raphaël)

The methodology is exemplified in detail on the Lie group of 3D rotations SO(3). It is well known that the tangent space of SO(3) at the identity matrix is the Lie algebra of anti-symmetric matrices AS(3). SO(3) is equipped with the standard bi-invariant metric which is the Frobenius inner product : $g(X,Y) = Tr(X^TY)$. The tangent space of SO(3) at an arbitrary matrix R is given by $R * AS(3)$ (or $AS(3) * R$).

For a matrix Lie group, the exponential map coincides with the matrix exponential. Moreover, the exponential map is defined for each $R \in SO(3)$, and is an application from the tangent space of SO(3) in R to SO(3).

Let $\mathbf{k} \in \mathbb{R}^3$ be a unit vector and:

$$\mathbf{K} = \begin{bmatrix} 0 & -k_z & k_y \\ k_z & 0 & -k_x \\ -k_y & k_x & 0 \end{bmatrix} \in AS(3)$$

Then,

$$\exp(\theta\mathbf{K}) = \sum_{k=0}^{\infty} \frac{(\theta\mathbf{K})^k}{k!} = I + \theta\mathbf{K} + \frac{1}{2!}(\theta\mathbf{K})^2 + \cdots$$

The characteristic polynomial P(t) of $\mathbf{K}$ is $P(t) = det(\mathbf{K} - t\mathbf{I})$ and the determinant can be computed by hand using Sarrus' formula. We get $P(t) = -(t^3 + t)$. Since, by the Cayley–Hamilton theorem, $P(\mathbf{K}) = 0$, this implies that :

$$\mathbf{K}^3 = -\mathbf{K}\,.\mathbf{K}^3 = -\mathbf{K}\,.$$

As a result, $\mathbf{K}^4 = -\mathbf{K}^2, \mathbf{K}^5 = \mathbf{K}$...

This cyclic pattern continues indefinitely, and so all higher powers of $\mathbf{K}$ can be expressed in terms of $\mathbf{K}$ and $\mathbf{K}^2$. Thus,

$$\exp(\theta\mathbf{K}) = I + \left(\theta - \frac{\theta^3}{3!} + \frac{\theta^5}{5!} - \cdots\right)\mathbf{K} + \left(\frac{\theta^2}{2!} - \frac{\theta^4}{4!} + \frac{\theta^6}{6!} - \cdots\right)\mathbf{K}^2$$

that is,

$$\exp(\theta\mathbf{K}) = I + (\sin\theta)\mathbf{K} + (1-\cos\theta)\mathbf{K}^2$$

.

Rodrigues' rotation formula states that if R $\in SO(3)$ is the rotation of angle θ around the axis $\mathbf{k}$, then $\mathbf{R} = \mathbf{I} + (\sin\theta)\mathbf{K} + (1-\cos\theta)\mathbf{K}^2$.

We have proven that $\exp(\theta\mathbf{K}) = \mathbf{R}$, which gives us an explicit formula for the exponential map from AS(3) to SO(3). Plugging $X = K/\theta$ in the above formula, the exponential map for a tangent vector $X \in AS(3)$ is given by :

$$\exp(X) = \begin{cases} I & \text{if } \theta = 0 \\ I + \dfrac{sin(\theta)}{\theta}X & \\ \quad + \dfrac{1-cos(\theta)}{\theta^2}X^2 & \text{if } \theta \in]0,\pi[\end{cases}$$

where $\theta = \sqrt{\frac{1}{2}\text{Tr}(X^T X)}$.

A geodesic $\gamma(t)$ starting at a point $R \in SO(3)$ with initial velocity RX is given by:

$$\gamma(t) = R\exp(tX)$$

The Lie group log map for a rotation matrix $R \in SO(3)$ is given by

$$\log R = \begin{cases} 0 & \text{if } \theta = 0 \\ \dfrac{\theta}{2\sin\theta}\left(R - R^{\mathsf{T}}\right) & \text{if } \theta \neq 0 \text{ and } \theta \in [-\pi,\pi] \end{cases}$$

with

$$\theta = \arccos\left(\frac{\text{Tr}(R)-1}{2}\right)$$

.

Given rotation matrices A and B,

$$d_g(A,B) := \left\|\log\left(A^{\mathsf{T}}B\right)\right\|_{\text{F}}$$

is the geodesic distance on the 3D manifold of rotation matrices.

If we want to solve the regression problem on a manifold by using a gradient descent algorithm, we have to minimize

$$f(R,\{R_i,w_i\}) = \frac{1}{2}\sum_i w_i d(R,R_i)$$

Its gradient at a point R is

$$\nabla_R f = -\sum_i w_i R\log(R^T R_i)$$

Given the estimate at step k $\hat{R}_k$, the update is $\hat{R}_{k+1} = \exp_{\hat{R}_k}(-\alpha\nabla_{\hat{R}_k} f)$ with α a step size.

3.1.3 Kernel Regression for Populations of Brain Images

The shape regression methodology will now be applied to study the effect of aging on brain shape from random design image data. We have observations of the form $\{t_i, I_i\}_{i=1\ldots N}$ where t_i is the age of patient i and I_i is a three-dimensional image that we can identify with the anatomical configuration of patient i. We're trying to compute the unknown function m that associates a representative anatomical configuration, and its associated image $\hat{I}$, with each age.

Let $\Omega \subset \mathbb{R}^3$ be the underlying coordinate system of the observed images I_i. We will work on this manifold rather than $\mathbb{R}^3$, as we want to use the structure of the brain images (if we do a mean of the images voxel-wise for example, the result will most likely not be a brain).

Thus, we represent anatomical differences in terms of transformations of the underlying image coordinates. This approach is common within the shape analysis literature ([18], [19]). The goal is to capture the large, natural geometric variability in the brain, so we represent shape change as the action of the group of diffeomorphisms, denoted by $\mathcal{H}$.

Let $\mathcal{H}$ be the group of diffeomorphisms that are isotopic to the identity. Each element $\phi : \Omega \to \Omega$

in $\mathcal{H}$ deforms an image in the following manner : $I_\phi(x) = I(\phi^{-1}(x))$.

We apply the theory of large deformation diffeomorphisms ([20], [21]) to generate deformations ϕ that are solutions to the Lagrangian ODEs $\frac{d}{ds}\phi_s(x) = v_s(\phi_s(x))$ for a simulated time parameter $s \in [0,1]$. The transformations are generated by integrating the time-varying velocity fields v_s forward in time. The chosen metric on $\mathcal{H}$ is $||v_s||_V^2 = \int_\Omega Av_s \cdot v_s dx$ with A a partial differential operator. The identity transformation of $\mathcal{H}$ is noted e. We define the distance between a diffeomorphism and the identity as:

$$d_\mathcal{H}(e,\phi)^2 = \min_{v:\frac{d}{ds}\phi_s = v_s(\phi_s)} \int_0^1 ||v_s||_V^2 ds$$

subject to $\phi(x) = x + \int_0^1 v_s(\phi_s(x))ds$ for all $x \in \Omega$.

The distance between two diffeomorphisms is $d_\mathcal{H}(\phi_1,\phi_2)^2 = d_\mathcal{H}(e, \phi_1^{-1} \circ \phi_2)^2$.

We can use this metric to define the distance between two images as :

$$d_\mathcal{I}(I_1,I_2)^2 = \min_{v:\frac{d}{ds}\phi_s = v_s(\phi_s)} \left[\int_0^1 ||v_s||_V^2 ds + \frac{1}{\sigma^2}||I_1(\phi^{-1}) - I_2||_{L^2}^2 \right]$$

where the second term represents the noise model of the image.

We can now regress a representative anatomical configuration, given the samples $\{t_i, I_i\}_{i=1...N}$:

$$\hat{I}_h(t) = \underset{I \in \mathcal{I}}{\text{argmin}} \left(\frac{\sum_{i=1}^n K_h(t-t_i) d_\mathcal{I}(I,I_i)^2}{\sum_{i=1}^n K_h(t-t_i)} \right)$$

Informally, at time t, the population can be represented by an image that is the closest to the images I_i whose associated times are close to t. The equation is solved with an iterative greedy algorithm as in [22].

3.1.4 Single-Subject Growth Model

Given several image observations J_t at different times t, we now seek the diffeomorphic flow g_t that flows through these images as time increases ([4]). It is given by

$$\underset{v:\dot{g}_t = v_t(g_t)}{\text{argmin}} \left[\int_0^1 ||v_t||_V^2 dt + \frac{1}{\sigma^2} \int_0^1 ||J_\alpha(g_t^{-1}) - J_t||_{L^2}^2 dt \right]$$

This gets us a diffeomorphic flow that is close to all the example images at all times, and whose norm in the $\mathcal{H}$ space isn't too important (the first term acts as a penalization). We use a discrete version of this equation to get an iterative solution for v_t, using gradient descent [23].

3.1.5 Step 2 : Population Growth Model (Raphaël)

To extend this growth model to a population growth model, we simply replace the collection of images J_t by the mean observed imagery for the population $\hat{I}_h(t)$ computed thanks to the manifold kernel regression estimator. A solution to this problem will yield the evolution of the shape of the brain for the average patient.

Once g_t is computed, we can take the log-determinant of its Jacobian to determine local geometric change in the population at a given time : it indicates an expansion if it's positive and a local contraction if it's negative.

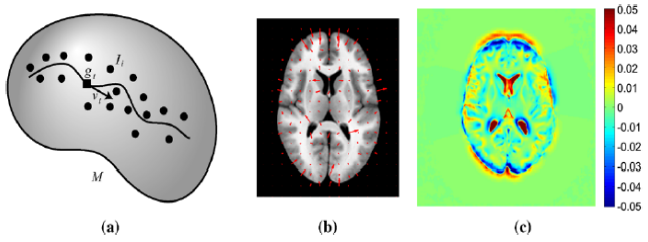

Figure 3

In Figure 3: (a) The diffeomorphism g_t quantifies the geometric change of $\hat{I}$ throughout the

growth period. v_t indicates the velocity of those changes. (b) The velocity field $v_t = \dot{g}_t$ is overlaid on the anatomical image. The arrows indicate instantaneous shape change at age t. (c) This colormap identifies regions of local expansion and contraction of the underlying anatomy at time t, with the method discussed in the paragraph above. Red indicates expansion; blue indicates contraction.

3.2 Results (Ariane)

3.2.1 On synthetic data

The synthetic data generated consists of bulls-eyes (3 concentric disks) where the radii are determined by :

$$r_1(t_i) = f_1(t_i) + \epsilon_i + \epsilon_{i,1}$$
$$r_2(t_i) = f_2(t_i) + \epsilon_i + \epsilon_{i,2}$$
$$r_3(t_i) = f_3(t_i) + \epsilon_i + \epsilon_{i,3}$$

where the ϵs are geometric noises. Some gaussian noise is also added to get more realistic images.

This provides a good proof of concept, but the issue with this data is that it does not do justice to the complexity of the human brain. Indeed, the gaussian geometric noise only modifies the radius of the disks, but does not change their general shape, which would correspond to brains of different global size but same shape of tissues. The core of the issue here being the shape changes, the bulls-eye images seem a bit simplistic.

3.2.2 On 3D MRI brain images

The main issue with the application here is the low amount of images in the dataset. Nowadays, we have much larger datasets available, like http://brain-development.org/ixi-dataset/ and http://fcon_1000.projects.nitrc.org/fcpClassic/FcpTable.html that have respectively more than 600 and 1200 brain MRIs. By retraining the model on those datasets, we might surely improve the accurracy and increase the robustness to individual variation.

3.3 Conclusion of the paper (Ariane)

One of the ideas of future works in the conclusion of the article was about the need of a method to quantify the descriptive trends found. This has been done by the company Quantib ([17]), that created this year a tool for healthy brain shape deformation analysis. Their method is similar to the one of the paper, with an additional step computing "morphology scores"/ Those scores are plotted as a function of age, and the variation in the population can be quantified using percentile curves that tell us which morphology score is to be expected at a certain age with a certain probability.

The other question was about the statistical significance of shape changes with age. In the case of the brain, it is partly answered in the article "Evolution of hippocampal shapes across the human lifespan" ([9]) where the deformation of the hippocampal shape and volume are statistically proven.

4 Further use of the article

(Antoine)

4.1 Patient-specific atlas of the brain

Ericsson et Al. 2008 [10] used the idea of this article to, propose a patient-specific atlas of the brain. Instead of comparing a subject with a generic population-specific atlas, the paper proposes for every subject of the cohort to build its own customized atlas. To that extent, the method uses also a kernel smoothing based on similarity with the other subjects of the cohort. This similarity can be based on the age, as in our case, but also other meta-data information such as sex, ethnicity or medical history.

4.2 Probabilistic atlas of the developing brain

Kuklisova-Murgasova et Al. 2010 [11] also used the idea of Kernel regression to create age-dependent maps for multiple brain structures. In this case, the model is applied in the prenatal context, when the deformation of the brain shape is much more significant. The other main difference is that the model has a probabilistic approach : estimated maps represent a tissue probability into the space.

4.3 Spatio-temporal atlas of the developing brain

Serag et Al. 2012 [12] also creates a spatio-temporal atlas with a Kernel regression in a prenatal context. A significant improvment regarding our initial paper is the use of a time-varying kernel width, in order to avoid being biased if the distribution of the cohort ages is not uniform.

5 Possible applications (Ariane)

One of the main issues of this article is the lack of visibility on the potential implications and uses of the brain growth model.

5.1 Medical application

Whereas simply observing the deformation due to brain aging is interesting, it might also be really useful to detect diseases like Alzheimer's. We can imagine that, by comparing the real evolution between to MRIs of a patient with the theoritical one, we might detect abnormal brain deformation that are the consequence of diseases such as Alzheimer's . Indeed, the hypothesis that brain age is a biomarker for neurodegenerative diseases and that Alzheimer's contain features correlated to accelerated brain aging is well established ([13, 14, 15]). The main issue with that method for the diagnosis of neurodegenerative diseases is that we need anterior MRIs of the patient to be able to estimate the theoritically normal current brain shape.

5.2 Example of non-medical application for shape regression

Shape regression can also be used for facial recognition that needs alignement. Instead of the brain shape changing with age, we study face shape changing with pose and facial expression: the goal is to identify faces with a different expression than what has previously been seen. New methods have been developed to that end, among which [7, 8]. Those are based on Recurrent Neural Networks that compute regressors in cascade. We can assume that we could also compute regressors that would describe the flow of deformation of the brain with aging like the studied paper from Davis, or converely use Davis' method to do face alignement.

6 Two related recent methods (Ariane)

6.1 Solution developed by Quantib

Quantib is a company doing Artificial Intelligence in Healthcare Solutions, and they developed a method to estimate the evolution of brain morphology with aging ([16]). The method is also in two steps, but is slightly different from the one of Davis et al. article: instead of computing an average brain per age range, they computed an overall average brain with group-wise image registration (so all brain images are weighted equally). The advantage is a better stability of the averaging, which could easily be biased in Davis' method.

6.2 Brain age estimation with MRIs using CNN

A more recent method, developed in March 2019 ([17]), predicts the physiological age of the brain from MRIs images. The differences with the studied article are in the method : Convolutional Neural Networks combined with Linear regression on the volume of segmented parts of the brain; and in the prediction: instead of trying to modelize the flow of deformation, we want to directly predict the age of the brain from an image.

However, the applications could be the same: detecting an abnormal shape of the brain for a certain age, which would imply a potential neurodegenerative disease. If the predicted age of the brain MRI of a new patient is over-evaluated, it might be linked to an abnormally fast brain aging and therefore Alzheimer's.

The results found by this article corroborate the brain aging correlation with neurodegenerative diseases hypothesis:

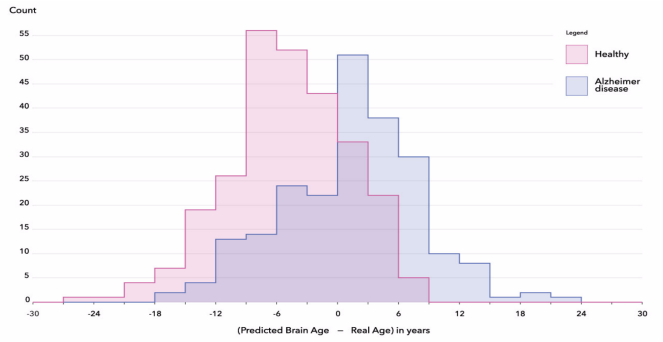

The distribution of the difference between the predicted and the reported subject age differ by 6 years on average between normal controls and Alzheimer's disease over the 489 patients of the ADNI database.

Figure 4: Results from [17]

References

[1] Olivier Clatz, Maxime Sermesant, Pierre-Yves Bondiau, Hervé Delingette, Simon K. Warfield, Grégoire Malandain, and Nicholas Ayache (October 2005). *Realistic Simulation of the 3-D Growth of Brain Tumors in MR Images Coupling Diffusion With Biomechanical Deformation*

[2] K. R. Swanson (October 2000). *A quantitative model for differential motility of gliomas in grey and white matter*

[3] Thompson, P. M., Giedd, J. N., Woods, R. P., MacDonald, D., Evans, A. C., & Toga, A. W. (2000). *Growth patterns in the developing brain detected by using continuum mechanical tensor maps. Nature, 404(6774), 190–193.*

[4] Miller, M. (2004). *Computational anatomy: shape, growth, and atrophy comparison via diffeomorphisms. NeuroImage, 23, S19–S33.*

[5] Nadaraya, E. A. (1964). *On estimating regression. Theory of Probability and its Applications, 10, 186–190.*

[6] Watson, G. S. (1964). Smooth *regression analysis. Sankhya, 26, 101–116.*

[7] W. Wang, S. Tulyakov, N. Sebe (March 2018). *Recurrent Convolutional Shape Regression* https://www.researchgate.net/publication/323502242_Recurrent_Convolutional_Shape_Regression

[8] Z. Cui, S. Xiao, Z. Niu, S. Yan, W. Zheng (April 2018). *Recurrent Shape Regression* https://www.researchgate.net/publication/324614646_Recurrent_Shape_Regression

[9] Yang X1, Goh A, Chen SH, Qiu A. (November 2013). *Evolution of hippocampal shapes across the human lifespan* https://www.ncbi.nlm.nih.gov/pubmed/22815197

[10] Anders Ericsson, Paul Aljabar, Daniel Rueckert (2008). *Construction of a Patient-Specific Atlas of the Brain: Application to Normal Aging*

[11] Maria Kuklisova-Murgasova, Paul Aljabar, Latha Srinivasan, Serena J. Counsell, Valentina Doria, Ahmed Serag, Ioannis S. Gousias, James P. Boardman, Mary A. Rutherford, A. David Edwards, Joseph V. Hajnal, Daniel Rueckert (2010). *A dynamic 4D probabilistic atlas of the developing brain*

[12] Ahmed Serag, Paul Aljabar, Gareth Ball, Serena J. Counsell, James P. Boardman, Mary A. Rutherford, A. David Edwards, Joseph V. Hajnal, Daniel Rueckert (2012). *Construction of a consistent high-definition spatio-temporal atlas of the developing brain using adaptive kernel regression*

[13] C. A. Raji, O. L. Lopez, L. H. Kuller, O. T. Carmichael, J. T. Becker (December 2015). *Age, Alzheimer disease, and brain structure* https://www.ncbi.nlm.nih.gov/pmc/articles/PMC2788799/

[14] C. Gaser, K. Franke, S. Klöppel, N. Koutsouleris, H. Sauer (June 2013). *BrainAGE in Mild Cognitive Impaired Patients: Predicting the Conversion to Alzheimer's Disease* https://journals.plos.org/plosone/article?id=10.1371/journal.pone.0067346

[15] J. H. Cole, R. Leech, D. J. Sharp (January 2015). *Prediction of brain age suggests accelerated atrophy after traumatic brain injury* https://onlinelibrary.wiley.com/doi/full/10.1002/ana.24367

[16] Quantib (March 2019). *How to measure the changing shape of the aging brain?* https://www.quantib.com/blog/how-to-measure-the-changing-shape-of-the-aging-brain

[17] J. H. Cole, R. Leech, D. J. Sharp (March 2019). *How to estimate the age of your brain with MRI data* https://medium.com/thelaunchpad/how-to-estimate-the-age-of-your-brain-with-mri-data-c60df60da95d

[18] Grenander, U., & Miller, M. I. (1998). *Computational anatomy: An emerging discipline.* Quarterly of Applied Mathematics, 56(4), 617–694.

[19] Miller, M., Banerjee, A., Christensen, G., Joshi, S., Khaneja, N., Grenander, U., & Matejic, L. (1997). *Statistical methods in computational anatomy.* Statistical Methods in Medical Research, 6, 267–299.

[20] Beg, M. F., Miller, M. I., Trouvé, A., & Younes, L. (2005). *Computing large deformation metric mappings via geodesic flows of diffeomorphisms.* International Journal of Computer Vision, 61(2), 139–157.

[21] Dupuis, P., & Grenander, U. (1998). *Variational problems on flows of diffeomorphisms for image matching.* Quarterly of AppliedMathematics, LVI(3), 587–600.

[22] Joshi, S., Davis, B., Jomier, M., & Gerig, G. (2004). *Unbiased diffeomorphic atlas construction for computational anatomy.* NeuroImage, 23, S151–S160. (Supplemental issue on Mathematics in Brain Imaging). http://www.sci.utah.edu/~gerig/publications/NeuroImage04-Joshi.pdf

[23] Miller, M. I., Trouve, A., & Younes, L. (2002). *On the metrics and Euler-Lagrange equations of computational anatomy.* Annual Review of Biomedical Engineering, 4, 375–405.